# FOREST STRUCTURE INFROMATION EXTRACTION FROM POARIMETRIC ALOS PALSAR DATA

PI No. 315

*Chen Erxue [1] Li Zengyuan [1] Tian Xin [1] Fan Fengyun[1]*

*[1] Institute of Forest Resources Information Technique, Chinese Academy of Forestry, PRC*

## 1. INTRODUCTION

Forest biomass and its change over time have long been considered as key characteristics of ecosystems. The knowledge about the amount and distribution of biomass is important not only for understanding the carbon budgets, but also for forest management and other land surface processes related to water and energy budget.

Taking the advantage of synthetic aperture radar (SAR) for mapping forest volume or above ground biomass in big area, many studies have been carried out to extract forest parameters information from SAR data. The techniques suitable for forest volume or biomass extraction include C-band InSAR ([2], [3], [4]), L- and P-band intensity ([5], [6]) and L-band ([7], [8]) and P-band [9] polarimetric interferometry SAR (POLinSAR). C-band InSAR coherence has been observed using ERS Tandem data to have good correlation with volume density, and the higher the volume density the lower the InSAR coherence. However, the relationship between L-band InSAR coherence is much more complex and needs to be further investigated. C-band SAR intensity saturates at very low biomass level, so only L- and P-band intensity were thought as suitable for forest biomass estimation. In case of SAR intensity only, P-band is the best for biomass estimation with the highest saturation level. Normally, L-band intensity saturates at 120-160 ton/ha of biomass. In the case of POLinSAR technique, many successful observations have been carried out using L-band data. ALOS PALSAR can provide L- band dual-polarization (HH, HV) intensity data and quad-polarization data, Radarsat-2 can provide C- band quad-polarization data and TerraSAR-X can provide high resolution dual-polarization SAR data, so multi-temporal dual-intensity, polarimetry, InSAR coherence and POLinSAR can be potentially used for land cover and forest parameters mapping.

In this report we focus on the investigation of ALOS PALSAR data for forest stand volume estimation, general land cover type classification over hilly area. The data processing and analysis results of the ALOS PALSAR POLinSAR dataset were also reported.

## 2. TEST SITES AND DATA

One test site located in ***Taian***, Shandong Province of China has been established, which covers ***Tai Mountain***, ***Tanan City***, Agricultural area and ***Culai Mountai****n*. Its geographic coordinate ranges from N35°59′ to 36°5′ and from E117°13′to 117°25′. The forest covering area of the test site is composed of ***Tai Mountain*** and ***Culai Mountain***, whose forest coverage rate is above 80%. There are two major forest types: *Black Locust* dominated forest and *Chinese Pine* dominated forest.

One remote sensing campaign has been carried out over this test site from April to June of 2005. The airborne sensor data acquired includes small footprint LiDAR, high spatial resolution color CCD and hyper-spectral data. One ortho-rectified color CCD image mosaic for the whole test site was produced. The DEM in map scale of 1:20 000 and forest component maps for the test site have been constructed. One scene of Landsat TM image covering the whole ***Taian*** district and one scene of SPOT5 image covering ***Culai*** test site are also available for aiding data analysis. Please note that we focus on ***Culai*** test site when talking about forest type classification and forest structure information extraction, while we use the whole area covering ***Tai Mountain***, ***Taian City*** and the agricultural regions as test site for general land cover type classification analysis.

Seven scenes of ALOS PALSAR level 1.1 data have been acquired. The major imaging parameters were listed in Tab. 1.

**Table1. The major imaging parameters for the PALSAR data**

| Imaging Date | Polarization | Incidence Angle(deg) |
|---|---|---|
| May 19, 2007 | Quad | 23.8 |
| June 21, 2007 | HH, HV | 38.7 |
| July 20, 2007 | HH, HV | 38.7 |
| Sept 21, 2007 | HH, HV | 38.7 |
| Oct. 20, 2007 | HH, HV | 38.7 |
| April 2, 2009 | Quad | 23.8 |
| May 18, 2009 | Quad | 23.8 |

Aimed to investigate the capability of PALSAR data for land cover classification and forest structure information estimation, ground true data were collected through field work from May to June of 2008. The high resolution airborne CCD image mosaic was used to identify each forest stands through manual interpretation. Some forest

stands were selected for field plot data measurement. The location of each stand was found according to its image feature in the high resolution CCD mosaic and GPS, and 1~4 plots were surveyed in each stand according to the coverage size and the structure of it. The volume density, mean height (*H*) and mean diameter at breast height of 1.3m (*DBH*) of each plot was calculated according to filed measurement of *H* and *DBH* for each tree of one plot, which we defined as plot level ground true data. The average value of all the plots filled into one stand was taken as the surveyed forest parameter for this stand, and this measurement is defined as forest stand volume in forest stand level. The total plot number of *Black Locust* forest is 75, and that for *Chinese Pine* is 69. Not all of the plots were really covered by the geocoded terrain corrected SAR images, so the effective plot number can change from image to image acquired in different date, but there exist at least 50 plots for the smallest image coverage case.

## 3. RESULTS AND ANALYSIS

### 3.1 Stand volume estimation using ALOS PALSAR

We have investigated the potential capability of ALOS PALSAR data for forest stand volume estimation in the ***Culai Mountain*** test site both in plot size (mapping unit size is 20m×20m) level and forest stand level (mapping unit size is the whole polygon area of one forest stand).

Before doing any analysis, we have to make the SAR images geocoded terrain corrected (GTC). For SAR image of mountain region, it is not possible to collect ground control points (GCPs) from the image directly, so the DEM simulated SAR image is used for GCPs collection and Range-Doppler geolocation model parameters refinement. The terrain radiometric correction (TRC) factor, layover and shadow mask image can also be produced during the SAR image simulation, which can be used for TRC processing of SAR intensity image and aiding for further data analysis.

In addition to PALSAR intensity of different polarizations, we also generated Cloude-Pottier H-Alpha-A decomposition parameters (Entropy, Alpha and A) for correlation analysis with forest stand volume. In plot size level, the correlation coefficient (R) of each SAR parameters to forest volume is shown in Fig.1. It shows that for ***Black Locust*** forest, HH, VV, HV, VH and HH/VV have negative correlation with volume density. HH is much more sensitive than VV and HV. HV/HH, Entropy and Alpha ( $\overline{\alpha}$ ) are the three parameters with R bigger than 0.4 (Fig.1).

Furthermore, the correlation coefficients in forest stand level were also analyzed. The trend is similar to the pixel level analysis result shown in Fig.1. The only difference is that the R value of dual-polarization ratio, Entropy and Alpha to forest stand volume increased to 0.6 above. We did the same analysis for ***Chinese Pine*** forest, in pixel level, all the R value is around 0.2, while in forest stand level some R value can increased to 0.6, but most of them are lower than 0.4.

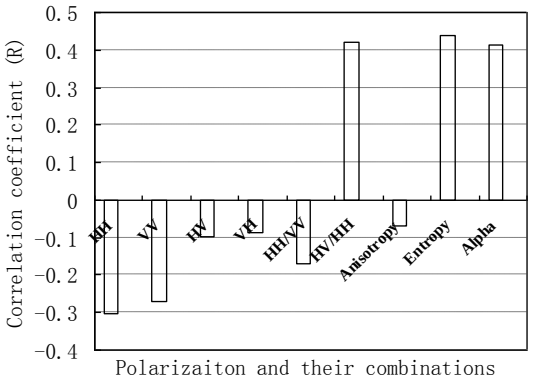


**Fig.1 Correlation coefficient between volume density and different polarization, their combinations and polarimetric decomposition parameter for *Black Locust* forest stand in plot size level**

The four dual-polarization images acquired in June, July, Sept. and Oct. 2007 were analyzed for HV/HH ratio, HV intensity and HH intensity after TRC processing, the R values for the two forest types and for each month are shown in Tab. 2. Although some images have signification correlation with forest stand volume from statistic point, but in general, we think the relationship is too weak to generate acceptable forest stand volume map.

**Table 2 Correlation coefficient between SAR parameters and forest stand volume in plot size level**

| Forest Type | Plot (N) | **Month** | After terrain radiometric correction(TRC) | | |
|---|---|---|---|---|---|
| | | | HV/HH | HV | HH |
| Black Locust | 55 | June | 0.292* | 0.174 | -0.109 |
| | 66 | July | 0.116 | 0.114 | 0.041 |
| | 55 | Sept. | 0.294* | -0.100 | -0.318* |
| | 66 | Oct. | 0.242* | -0.155 | -0.315* |
| Chinese Pine | 64 | June | -0.013 | 0.026 | 0.035 |
| | 58 | July | 0.164 | -0.078 | -0.179 |
| | 64 | Sept. | -0.026 | 0.105 | 0.118 |
| | 58 | Oct. | -0.009 | 0.089 | 0.092 |

**Note: *stand for the correlation is significant.**

### 3.2 Land cover types classification using ALOS PALSAR quad-polarization data

We have compared the performance of several unsupervised polarimetric SAR land cover type classification methodologies using the PALSAR quad-polarization data acquired in May 19, 2007. Further more, in 2009, we got one pair of quad-polarization InSAR data. After registered the slave image (May) to the master

image (April), we use the same training AOIs for supervised polarimetric SAR Wishart classification applied to master and slave image separately, and the information classes we defined include water body, bare soil, urban, crop fields, forest and layover. All the training AOIs were carefully defined with land use map, Landsat ETM+ image, SPOT5 image, the CCD mosaic and ground visit experience as reference. Fig.2 shows the master image, classification result and the AOIs used for training the classifier, the class legend is shown on the top of Fig.2 right plate. Tab.3 listed the classification accuracy for each land cover type. Because master and slave image has certain correlation with each other, so the classification accuracy has no significant difference. It can be concluded that ALOS PALSAR polarimetric SAR data is very useful for general land cover type mapping, although it is not suitable for forest types mapping in hilly regions.

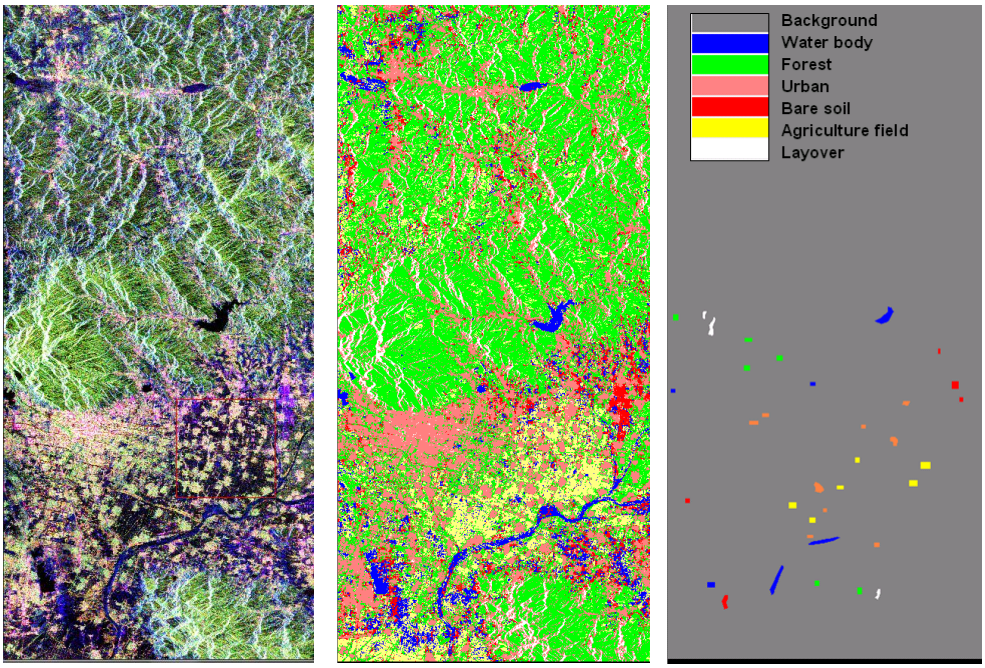


**Fig.2 Master image shown in Pauli base (Left), classification result (Middle) and AOIs with legend (Right)**

**Table 3. Classification accuracy of quad-polarization images acquired with 46 days time difference**

| Imaging date | Land cover type classification accuracy (%) | | | | | | |
|---|---|---|---|---|---|---|---|
| | Water Body | Forest | Urban | Bare Soil | Agri. field | Layover | Mean |
| April 2 | 79.68 | 95.00 | 98.78 | 77.88 | 94.99 | 86.07 | 88.73 |
| May 18 | 83.85 | 94.35 | 98.27 | 84.65 | 93.79 | 86.07 | 90.16 |

### 3.3 POLinSAR dataset analysis for forest height inversion

Taking PALSAR April 2 image as master and May 18 image as slave, we choose HH polarization for image to image registration processing. The offset points between master HH and slave HH image is used to construct the image registration model, which was used to resample the slave images of the four polarizations to the master images with common bandwidth filtering. The offset points and the SAR sensor state vectors are combined to estimate the baseline information. All the processing above carried out in SLC domain. The estimated baseline length is 226.9m, the cross track length is 206.1m and the normal baseline is 94.9m; Parallel component length is 163.5m and the perpendicular component is 157.3m.

After registration, we constructed two scattering matrix $[S_2]_{Master}$ and $[S_2]_{Slave}$ that are precisely overlaid to each other. Then, we import the two $[S_2]$ matrix into PolSARPro to construct one multi-looked $[T_6]$ matrix (7 pixels in azimuth×1 pixel in range) and do the flat earth phase removal processing and applying Lee filter of window size 5 pixels×5 pixels to it. The effective wave number (kz) image was computed from the baseline and satellite position information. Fig.3 shows the interferogram of three polarizations (HH to HH, HV to HV and VV to VV). Fig.4 shows the amplitude of coherences of the three polarizations.

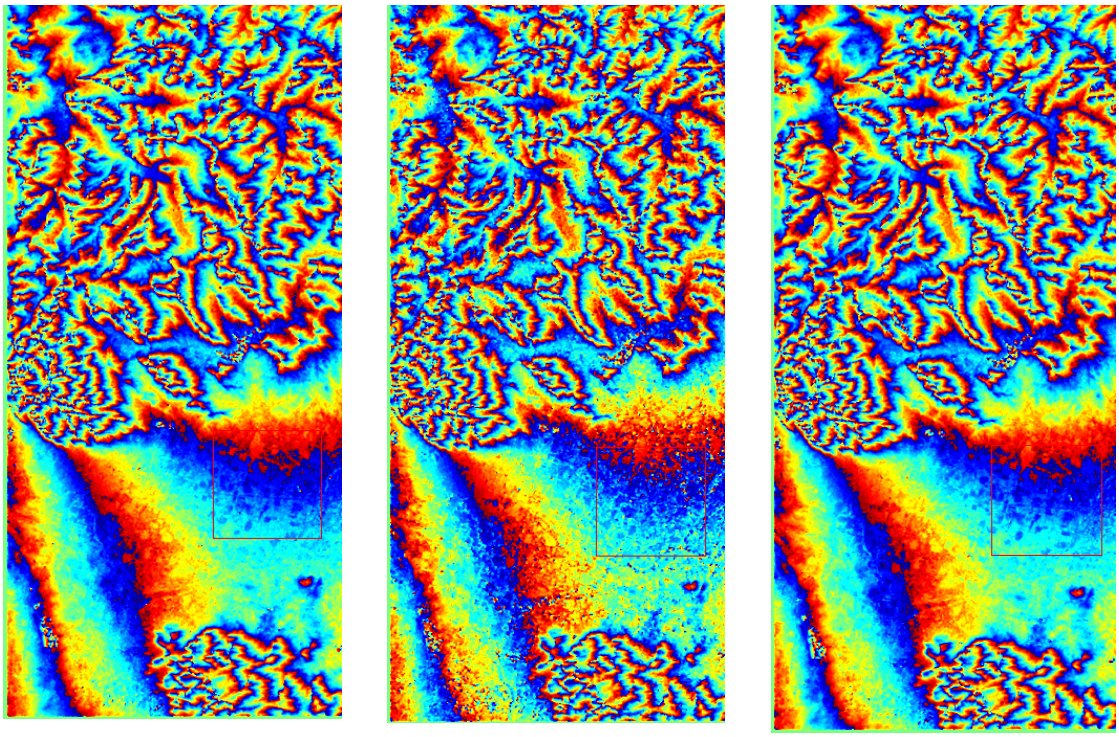

**Fig.3 Interferogram of HH to HH (left), HV to HV (middle) and VV to VV (right)**

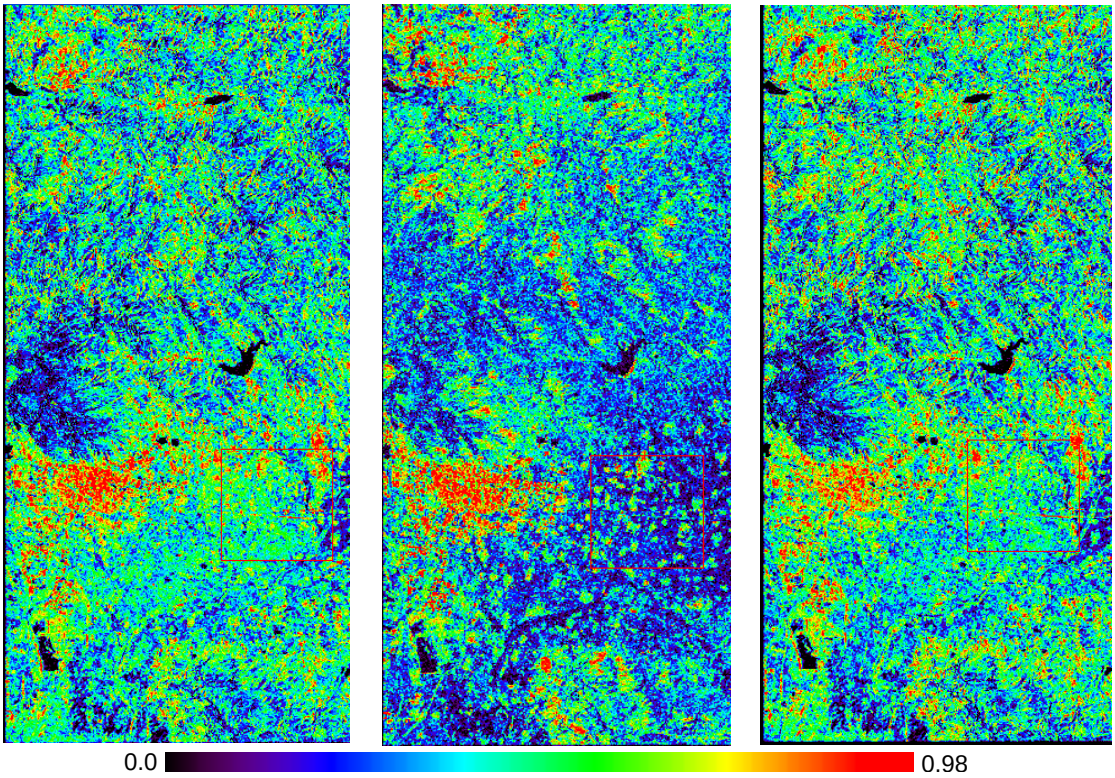


**Fig.4 The amplitude of the coherences of HH to HH (left), HV to HV (middle) and VV to VV (right)**

The HH to HH coherence and VV to VV coherence image are of the similar feature (Fig.4), they show us that the water body is of the lowest coherence amplitude, the urban area (***Taian City*** below the ***Tai Mountain***) is of the highest coherence. The most parts of the ***Tai Mountain*** are of low coherence with blue color. However, the most part of ***Culai Mountain*** is of middle coherence that is the big difference compared with the ***Tai Mountain***. In the view of HV to HV coherence, the mean value of it is lower than HH to HH and VV to VV coherence, however, in the mountain forest region, there are more pixels to be of high coherence than in the copolarization coherence images. The agricultural fields are of relatively low coherence than in copolarization coherence image, because that HV mainly interacts with the crop canopy which can change dramatically in 46 days, while HH or VV interacts with ground surface, which is much more stable in 46 days. But in ***Culai Mountain***, we can find some areas are of very high coherence, while we know that these areas should be forest covered. It is difficult to explain the strange results, keeping in mind that the temporal baseline is 46 days and the topography is very complex here. Tab.4 listed the amplitude statistic for the six kinds of coherence: HH to HH, HV to HV, VV to VV, Optimum coherence 1, 2 and 3. The mean coherence amplitude changes from 0.193 to 0.494, the stand deviation is less than 0.16, so the coherence of this POLinSAR dataset can be considered as very low. We have tried to inverse the forest height from this dataset, but not successfully, most of the pixels in ***Culai Mountain*** are masked out during the inversion. Further analysis of this dataset for any possible advantages we can get from its interferometic information is still ongoing, for examples, if we can improve land cover classification accuracy of POLSAR with the help of coherence information.

**Table 4. The amplitude statistic for six kinds of coherence**

| Coherence Type | Coherence amplitude image statistic | | | |
|---|---|---|---|---|
| | Minimum | Mean | Maximum | Stand deviation |
| HH to HH | 0.000 | 0.396 | 0.982 | 0.155 |
| HV to HV | 0.000 | 0.246 | 0.976 | 0.126 |
| VV to VV | 0.000 | 0.390 | 0.977 | 0.151 |
| Optimum 1 | 0.000 | 0.494 | 1.000 | 0.146 |
| Optimum 2 | 0.000 | 0.322 | 1.000 | 0.141 |
| Optimum 3 | 0.000 | 0.193 | 1.000 | 0.141 |

### 3.4 Forest stand stem volume estimation using quad-polarization PALSAR data and LiDAR data

#### 3.4.1 LiDAR data & forest canopy height information

The airborne sensor data acquired includes small footprint LiDAR of low density (0.39 points/$m^2$), Fig 5. shows the flight route and the laser point cloud data of the Culai Mountain. High spatial resolution color CCD image mosaic (0.5m×0.5m) is shown as the background of Fig 6., and the vector (polygons) layer is the boundaries of each forest stand manually digitized from the CCD mosaic image. The digital elevation model (DEM) (Fig.7) is obtained by interpolating the classified LiDAR ground points, and the digital surface model (DSM) is generated by interpolating all LiDAR points classified as forest vegetation. The normalized crown height model (Canopy Height Model, CHM) (Fig.8) is the difference between DSM and DEM.

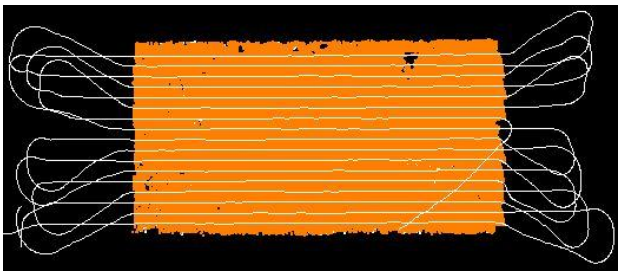

**Fig. 5 Flight route and the laser point cloud data**

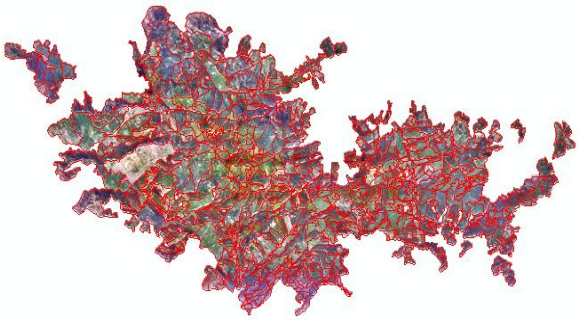

**Fig.6 Vector layer of forest stand boundaries overlaid on the high spatial resolution CCD mosaic image**

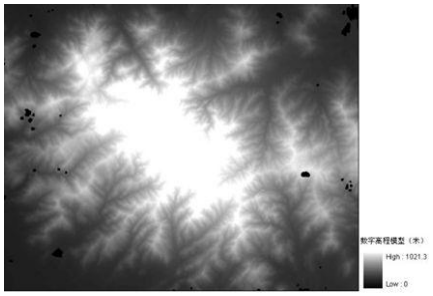

**Fig.7 Digital elevation model derived from LiDAR**

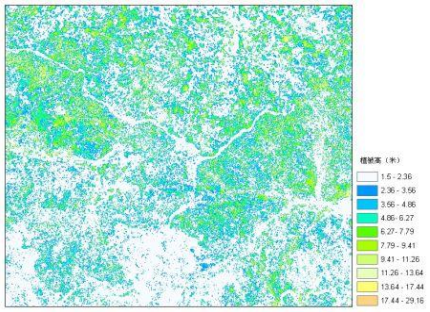

**Fig.8 Canopy height model derived from LiDAR**

### 3.4.2 Forest stand volume estimation by combined use of SAR and LiDAR derived forest canopy height

Forest stand stem volume is estimated based on LiDAR and polarimetric SAR data using multiple-stepwise logistic regression and field measured plot data in forest stand level. According to the sensitivity of backscattering coefficient and polarimetric decomposition parameter to forest stand volume, the following linear regression models was used to establish the relationship between forest stand volume and remote sensed parameters:

$$\ln V = \beta_0 + \beta_1 \ln h_{Mean} + \beta_2 \sigma^0_{hv/hh} + \beta_3 \sigma^0_{vh/hh} + \beta_4 \sigma^0_{hv/vv} + \beta_5 \sigma^0_{vh/vv} + \beta_6 H + \beta_7 \alpha + \varepsilon \quad (1)$$

$$\ln V = \beta_0 + \beta_1 \ln h_{Mean} + \beta_2 \sigma^0_{hv/hh} + \beta_3 \sigma^0_{vh/hh} + \beta_4 \sigma^0_{hv/vv} + \beta_5 \sigma^0_{vh/vv} + \beta_6 H + \beta_7 \alpha + \varepsilon \quad (2)$$

Where $V$ is forest stand volume ($m^3$/ha); $h_{Mean}$ is the mean forest canopy height extracted from the LiDAR CHM image; and $\sigma^0_{hv/hh}, \sigma^0_{vh/hh}, \sigma^0_{hv/vv}, \sigma^0_{vh/vv}, H, \alpha$ are polarmetric parameters ; $\varepsilon$ is a normally distributed error term [$\varepsilon \sim N(0, 1)$]. The final *Black Locust* and *Chinese Pine* volume estimation model is shown as equation (3) and (4) respectively, with the RMSE of 20.06$m^3$/ha for *Black Locust* and 24.73$m^3$/ha for *Chinese Pine*.

$$\ln V = 7.289 + 0.744 \ln H_{Mean} + 0.405\sigma^0_{vh/hh} + 0.016\sigma^0_{hv/vv} - 0.049\alpha \quad (3)$$

$$\ln V = 9.457 + 0.822 \ln H_{Mean} + 0.290\sigma^0_{hv/hh} + 0.163\sigma^0_{hv/vv} - 0.095\alpha \quad (4)$$

One forest stand volume map for the whole test sits has been produced (Fig.9) using the established models.

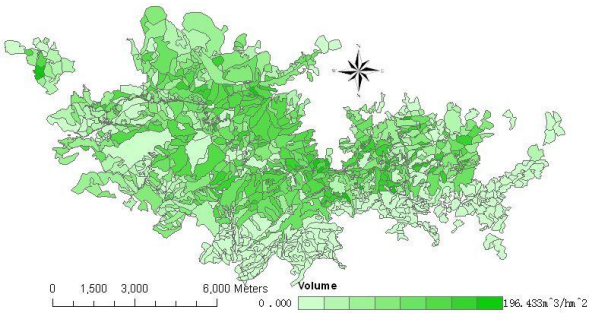


**Fig.9 Forest stand volume distribution map estimated from polarimetric SAR parameters and LiDAR derived forest canopy height**

## 4. CONCLUSIONS

Through this study we have found that the current terrain radiometric correction model has limited potential for hilly forest stand volume estimation using L-band SAR data, new correction methodology need to be developed. One temporal PALSAR quad-polarization data is very useful for mapping general land cover types, but adding another image of 46 days time difference may not improve classification accuracy significantly; ALOS PALSAR repeat pass (46 days) POLinSAR data is of very low coherence, preliminary results shows that it is difficult to inverse forest height from it. Combining LiDAR measurement and SAR parameters (polarization ratio and $\overline{\alpha}$ ), the regression model for estimating forest stand volumes have been established, and one forest stand volume map for the whole test site can be produced, with the RMSE of 20.06$m^3$/ha for *Black Locust* and 24.73$m^3$/ha for *Chinese Pine*.

## 6. REFERENCES


[1] Häme, T., Salli, A., & Lahti, K. (1992). Estimation of carbon storage in boreal forest using remote sensing data, Pilot study. In M. Kanninen, & P. Anttila (Eds.), The Finnish programme on climate change, Progress report. Publications of the Academy of Finland, vol. 3/92 (pp. 250-255). Helsinki, Finland: VAPK publishing.

[2] Luckman, A., Baker, J., & Wegmuller, U. (2000). Repeat-pass interferometric coherence measurements of disturbed tropical forest from JERS and ERS satellites. Remote Sensing of Environment. 73, 350-360

[3] Fransson, J., Smith, G., Askne, J., & Olsson, H. (2001). Stem volume estimation in boreal forests using ERS-1/2 coherence and Spot XS optical data. International Journal of Remote Sensing, 22(14), 2777-2791.

[4] Paulliainen, J., Engdahl, M., & Hallikainen, M. (2003). Feasibility of multi-temporal interferometric SAR data for stand-level estimation of boreal forest stem volume. Remote Sensing of Environment, 85, 397-409.

[5] Le Toan T., Beaudoin A., Riom J., & Guyon D. Relating forest biomass to SAR data. IEEE Trans. Geosci. Remote Sensing, 1992, 30: 403-411.

[6] Ranson K. J., Sun G. Mapping biomass of Northern forest using multifrequency SAR data. IEEE Trans. Geosci. Remote Sensing, 1994, 32: 388-396.

[7] Papathanassiou K P, Cloude S R. 2001. Single baseline polarimetric SAR interferometry. IEEE Trans. Geosci. Remote Sens., 39(11): 2352-2363

[8] Cloude S R, Papathanassiou K P. 2003. Three- stage inversion process for polarimetric SAR interferometry. IEE Proc. Radar Sonar Navig, 150 (3): 125-134

[9] Dubois F. P., Angelliaume S., Souyris J. C., Garestier F., Champion I., The Specificity of P band POLINSAR data over vegetation, 2007, POLINSAR Workshop, ESRIN Italy.